



Evidence for Innate and Adaptive Immune Responses in a Cohort of Intractable Pediatric Epilepsy Surgery Patients

Geoffrey C. Owens^{1*}, Alejandro J. Garcia², Aaron Y. Mochizuki^{2,3}, Julia W. Chang^{1,4}, Samuel D. Reyes¹, Noriko Salamon⁵, Robert M. Prins^{1,6,7,8}, Gary W. Mathern^{1,4,7,9} and Aria Fallah^{1,7,9}

¹ Department of Neurosurgery, David Geffen School of Medicine, University of California, Los Angeles, Los Angeles, CA, United States, ² Division of Hematology Oncology, Department of Medicine, David Geffen School of Medicine, University of California, Los Angeles, Los Angeles, CA, United States, ³ Department of Pediatrics, David Geffen School of Medicine, University of California, Los Angeles, Los Angeles, CA, United States, ⁴ Intellectual and Developmental Disabilities Research Center, David Geffen School of Medicine, University of California, Los Angeles, Los Angeles, CA, United States, ⁵ Department of Radiological Sciences, David Geffen School of Medicine at the University of California, Los Angeles, Los Angeles, CA, United States, ⁶ Department of Molecular and Medical Pharmacology, David Geffen School of Medicine, University of California, Los Angeles, Los Angeles, CA, United States, ⁷ Brain Research Institute, David Geffen School of Medicine, University of California, Los Angeles, Los Angeles, CA, United States, ⁸ Parker Institute for Cancer Immunotherapy, David Geffen School of Medicine, University of California, Los Angeles, Los Angeles, CA, United States, ⁹ Mattel Children's Hospital, David Geffen School of Medicine, University of California, Los Angeles, Los Angeles, CA, United States

OPEN ACCESS

Edited by:

Roland S. Liblau,
Institut National de la Santé et de la
Recherche Médicale (INSERM),
France

Reviewed by:

Catharina C. Gross,
University of Münster, Germany
Rishein Gupta,
University of Texas at San Antonio,
United States

*Correspondence:

Geoffrey C. Owens
geoffreyowens@mednet.ucla.edu

Specialty section:

This article was submitted to
Multiple Sclerosis and
Neuroimmunology,
a section of the journal
Frontiers in Immunology

Received: 15 September 2018

Accepted: 15 January 2019

Published: 29 January 2019

Citation:

Owens GC, Garcia AJ, Mochizuki AY,
Chang JW, Reyes SD, Salamon N,
Prins RM, Mathern GW and Fallah A
(2019) Evidence for Innate and
Adaptive Immune Responses in a
Cohort of Intractable Pediatric
Epilepsy Surgery Patients.
Front. Immunol. 10:121.
doi: 10.3389/fimmu.2019.00121

Brain-infiltrating lymphocytes (BILs) were isolated from resected brain tissue from 10 pediatric epilepsy patients who had undergone surgery for Hemimegalencephaly (HME) ($n = 1$), Tuberous sclerosis complex (TSC) ($n = 2$), Focal cortical dysplasia (FCD) ($n = 4$), and Rasmussen encephalitis (RE) ($n = 3$). Peripheral blood mononuclear cells (PBMCs) were also isolated from blood collected at the time of the surgery. Cells were immunostained with a panel of 20 antibody markers, and analyzed by mass cytometry. To identify and quantify the immune cell types in the samples, an unbiased clustering method was applied to the entire data set. More than 85 percent of the CD45⁺ cells isolated from resected RE brain tissue comprised T cells; by contrast NK cells and myeloid cells constituted 80–95 percent of the CD45⁺ cells isolated from the TSC and the FCD brain specimens. Three populations of myeloid cells made up >50 percent of all of the myeloid cells in all of the samples of which a population of HLA-DR⁺ CD11b⁺ CD4⁻ cells comprised the vast majority of myeloid cells in the BIL fractions from the FCD and TSC cases. CD45RA⁺ HLA-DR⁻ CD11b⁺ CD16⁺ NK cells constituted the major population of NK cells in the blood from all of the cases. This subset also comprised the majority of NK cells in BILs from the resected RE and HME brain tissue, whereas NK cells defined as CD45RA⁻ HLA-DR⁺ CD11b⁻ CD16⁻ cells comprised 86–96 percent of the NK cells isolated from the FCD and TSC brain tissue. Thirteen different subsets of CD4 and CD8 $\alpha\beta$ T cells and $\gamma\delta$ T cells accounted for over 80% of the CD3⁺ T cells in all of the BIL and PBMC samples. At least 90 percent of the T cells in the RE BILs, 80 percent of the T cells in the HME BILs and 40–66 percent in the TSC and FCD BILs comprised

activated antigen-experienced (CD45RO⁺ HLA-DR⁺ CD69⁺) T cells. We conclude that even in cases where there is no evidence for an infection or an immune disorder, activated peripheral immune cells may be present in epileptogenic areas of the brain, possibly in response to seizure-driven brain inflammation.

Keywords: brain, epilepsy, inflammation, peripheral immune cells, mass cytometry (CyTOF)

INTRODUCTION

It has been estimated that by 15 years of age, approximately one percent of children will have experienced at least one seizure (1). For reasons that may not always be understood ~10% of children go on to develop medically refractory epilepsy, which is defined as a failure of two or more antiepileptic drugs to control seizures, and at least one seizure per month for ≥ 18 months (2). Recurrent seizures may severely impair a child's cognitive development leading to lifelong learning and behavioral difficulties. For children with drug-resistant epilepsy, surgery may be the only option to obtain seizure freedom, but will result in neurological deficits if the zone of resection involves eloquent cerebral cortex.

Many of the children who are candidates for epilepsy surgery suffer from rare neurological disorders including Rasmussen encephalitis (RE), Tuberous Sclerosis Complex (TSC), Focal Cortical Dysplasia (FCD), and Hemimegalencephaly (HME). RE patients present with partial (focal) seizures; magnetic resonance images (MRI) may indicate inflammation and atrophy in the affected cerebral hemisphere (3). The inflammation may spread through the affected cerebral hemisphere, but generally does not cross over to the contralateral hemisphere (4). Histopathological examination of resected brain tissue and brain biopsies show T cells in perivascular spaces, leptomeninges, and in small clusters scattered throughout the affected gray and white matter (5, 6). Clonally focused T cells have been found in resected RE brain tissue strongly implicating an antigen driven immune response in disease etiology (7–10).

In TSC patients, germ line and somatic dominant loss of function mutations in the genes encoding hamartin (TSC1) or tuberin (TSC2) can cause the development of benign tumors and, abnormally differentiated cortical neuronal progenitors that may cause focal seizures (11). Tuberin and hamartin are components of a complex that regulates the activity of the protein kinase, mTOR (12). Similarly, FCD and HME can be caused by activating somatic mutations in the MTOR gene, and in genes that regulate mTOR activity (13–15). Histopathological examination of resected brain tissue and analysis of RNA transcripts has shown that FCD and TSC lesions may be associated with an inflammatory reaction (11, 16–19).

In the present study we report on the characterization, by mass cytometry, of brain-infiltrating lymphocytes (BILs) isolated from surgical resections of epileptogenic tissue to treat FCD, TSC, and HME, as well as RE, and of peripheral blood mononuclear cells (PBMCs) prepared from blood collected at the time of surgery from the same cases. Immune cell profiling showed that activated T cells were present in brain tissue from all of the cases examined, and that the relative abundance of adaptive and innate lymphoid

cells, and myeloid cells markedly differed between the RE and non-RE cases.

METHODS

Patient Cohort

Under UCLA IRB approval (IRB#18-000154) brain tissue and blood were collected at surgery as part of UCLA's Pediatric Epilepsy Surgery Program. All of the patients or their parents or legal guardians provided informed consent for the use of the surgical remnant and blood for research purposes. All specimens were collected using the same standard operating procedures. De-identified patient information including age at seizure onset, age at surgery, gender, and affected cerebral hemisphere was collected with informed consent (Table S1).

Isolation of Peripheral Blood Lymphocytes and Brain-Infiltrating Lymphocytes

PBMCs were isolated by density gradient centrifugation using Ficoll-Paque PLUS (GE Healthcare, Piscataway, NJ). BILs were isolated from collagenase-treated brain tissue by fractionation on a step gradient (20). Briefly, brain tissue was diced manually on ice in dissociation solution (HBSS with 20 mM HEPES pH 7.0, 5 mM glucose, and 50 U/ml penicillin/streptomycin). Tissue fragments were incubated with agitation at room temperature overnight in dissociation solution containing 0.5 mg/ml Type IV collagenase (Worthington Biochemical Corp., Lakewood, NJ) and 5% filtered human serum (Mediatech Inc., Manassas, VA). The dissociated tissue was fractionated on a 30%:70% Percoll[®] (SigmaAldrich, St. Louis, MO) step gradient in RPMI containing 20 mM HEPES. PBMCs and BILs were cryopreserved in 90% human serum /10% DMSO.

Multiparameter Mass Cytometry

The panel comprised the following markers: CD45 (89Y or 154Sm), CD196 (141Pr), CD19 (142Nd), CD69 (144Nd), CD4 (145Nd), CD8 (146Nd), CD25 (149Sm), CD103 (151Eu), CD45RA (155Gd), CD183 (156Gd), CD56 (163Dy), CD45RO (164Dy), CD16 (165Ho), TCR $\gamma\delta$ (168Er), CD3 (170Er), CD195 (171Yb), HLA-DR (174Yb), CD194 (175Yb), CD127 (176Yb), and CD11b (209Bi). All metal-tagged antibodies (Abs) were obtained from Fluidigm (San Francisco, CA) except the CD8 and TCR $\gamma\delta$ antibodies, which were conjugated in-house. PBMCs and BILs were stained according to Fluidigm's protocol. In brief, cells were thawed, and washed in phosphate-buffered saline (PBS); prior to staining BILs were filtered through a 40 μ m sieve to remove any aggregates. Cells were resuspended in 1 ml of PBS and stained for 5 min with 1 μ M Cisplatin. After quenching the staining with Maxpar[®] cell staining buffer (Fluidigm), cells

were incubated with the cocktail of Abs in 100 μ l of Maxpar[®] cell staining buffer for 30 min at room temperature. The Ab cocktail for staining PBMCs contained the CD45 Ab conjugated to Samarium 154 (154Sm) while the BIL Ab cocktail contained the CD45 Ab tagged with Yttrium 89 (89Y). Following two wash steps, cells were fixed overnight at 4°C in Maxpar[®] fixation and permeabilization buffer containing 0.125 μ M Intercalator-Ir (Fluidigm). BILs and PBMCs from the same surgery were combined at this point and washed twice with Maxpar[®] cell staining buffer and a further two times with water. Having barcoded the BILs and PBMCs with a different metal-conjugated CD45 Ab it was possible to analyze them as single sample, thus the larger number of PBMCs served as a carrier for the smaller number of BILs that were isolated from brain tissue. Cells were resuspended in 10 percent EQ[™] Four Element Calibration Beads (Fluidigm) containing Cerium (140/142Ce), Europium (151/153Eu), Holmium (165Ho), and Lutetium (175/176Lu). Samples were acquired on a Helios[®] cytometry time of flight (CyTOF) system (Fluidigm) at an event rate of 300–500 events/s. Post-acquisition data normalization was done using bead-based normalization in the CyTOF software. Prior to analysis, data were gated to eliminate normalization beads, debris, dead cells, and doublets.

The analysis of FCS files was initially carried out using Cytobank (21). For each surgery case, the marker expression on the BILs was resolved by first gating live singlets on CD45 (89Y). Conversely marker expression on PBMCs was resolved by first gating on CD45 (154Sm). The data were then split into two separate FCS files using software tools in Cytobank (21). To define subsets of immune cells in each BIL and PBMC population, the entire high dimensional dataset (comprising 20 FCS files) was converted into a matrix of pair-wise similarities by implementing the t-based stochastic neighbor embedding (t-SNE) algorithm, followed by a density-based clustering method (ClusterX) (22). The resulting 2-D plots from this procedure were exported to CorelDraw2017 as portable document format files (Corel Corporation, Ottawa, Canada). Individual FCS files were analyzed using FlowJo[®] software (FlowJo LLC, Ashland, OR); 2-D contour plots were exported as scalable vector graphic (svg) files to CorelDraw2017. The median level of expression of each marker was used to assign a phenotypic identity to each cluster. Heat maps were generated using Morpheus software (www.broadinstitute.org) and exported to CorelDraw2017 as svg files. Principal component analysis (PCA) was performed using PAST software (https://palaeo-electronica.org/2001_1/past/issue1_01.htm).

RESULTS

PBMCs and BILs isolated from 10 pediatric epilepsy cases were analyzed by CyTOF using a panel of antibodies designed to identify populations of adaptive lymphoid cells, innate lymphoid cells, and myeloid cells. Implementing the mass cytometry data analysis pipeline developed by Chen et al. (21) generated 46 clusters, corresponding to putatively distinct populations of

CD45⁺ cells (**Figure 1**). Clusters were classified as T cells, NK cells, and myeloid cells based on the relative expression of 19 immune cell markers. Immune cell clusters were divided into a CD3⁺ ($n = 30$, median CD3 expression values of 4.648–6.283) and a CD3[−] group ($n = 16$, median expression values of 0.001–0.81). The CD3⁺ group was subdivided into subsets of CD4, CD8, and $\gamma\delta$ T cells based on the level of expression of these three phenotypic markers (**Figure 2**). The CD3[−] group was further divided into five NK cell subsets, ten myeloid and one B cell population based on the expression of CD56 and CD19 (**Figure 2; Table S2**).

Visual inspection of the t-SNE plots (**Figure 1**) showed that there were clear differences between the BILs from each surgical case compared with the corresponding PBMCs. On the other hand, the profiles of BILs from the two TSC (Case IDs 460 and 462) and the four FCD cases (Case IDs 475, 490, 494, and 495) appeared to be very similar and distinct from the three RE cases (Case IDs 472, 484, and 497), and dissimilar from the HME (Case ID 485), which appeared more similar to the RE cases. Principal components analysis based on the relative abundance of all of the clusters in each sample (percentages of CD45⁺ cells) confirmed this observation, and also showed that the immune cell profiles of PBMCs from all of the cases were very similar (**Figure 3**). From the magnitude of the PCA loading values (**Table S3**), Clusters 1 and 8 accounted for the largest amount of variance in the first component, thus, the relative numbers of NK and myeloid cells in the BIL fractions appears to explain in large measure the observed difference between the TSC and FCD BILs compared with the RE and HME BILs. As summarized in **Figure 4**, CD45⁺ cells from the FCD and TSC brain tissue specimens comprised far more NK cells and myeloid cells than CD45⁺ RE BILs, which in agreement with previous studies (5, 6, 20, 23), were predominantly CD8⁺ $\alpha\beta$ T and $\gamma\delta$ cells, The HME BILs comprised approximately equal numbers of T cells, NK cells and myeloid cells.

Three populations of myeloid cells (Clusters 1, 7, and 45) (**Figure 2**) made up >50 percent of all of the myeloid cells in all of the samples (**Figure 5; Table S4**). The Cluster 1 myeloid population comprised the vast majority of CD11b⁺ cells in the BIL fractions from the FCD and TSC cases (**Figure 5**), whereas Cluster 7 CD11b⁺ myeloid cells were more abundant in two of the three RE BIL fractions (Case IDs 472 and 484), and in all of the PBMCs (**Figure 5**). The only other marker that defined the Cluster 1 population was HLA-DR, thus it was not possible to assign a definitive phenotype to cells in this population, but they are likely to be macrophages. Likewise, Cluster 7 cells, which are CD3[−] CD4^{lo} could constitute a dendritic cell or monocyte population, but additional markers are also required to adequately define this population.

Cluster 3 NK cells are CD56⁺ CD45RA⁺ HLA-DR[−] CD11b⁺ CD16⁺ (**Figure 2**), and constituted the major population of NK cells in the blood from all of the cases (**Figure 5**). This subset also comprised the majority of NK cells that were found in BILs from the resected RE and HME brain tissue (**Figure 5**). By contrast, Cluster 8 NK cells, defined as CD56⁺ CD45RA[−] HLA-DR⁺ CD11b[−] CD16[−] (**Figure 2**) comprised 86–96 percent of the NK cells isolated from the FCD and TSC brain tissue (**Figure 5; Table S4**). We confirmed the existence of Cluster 3

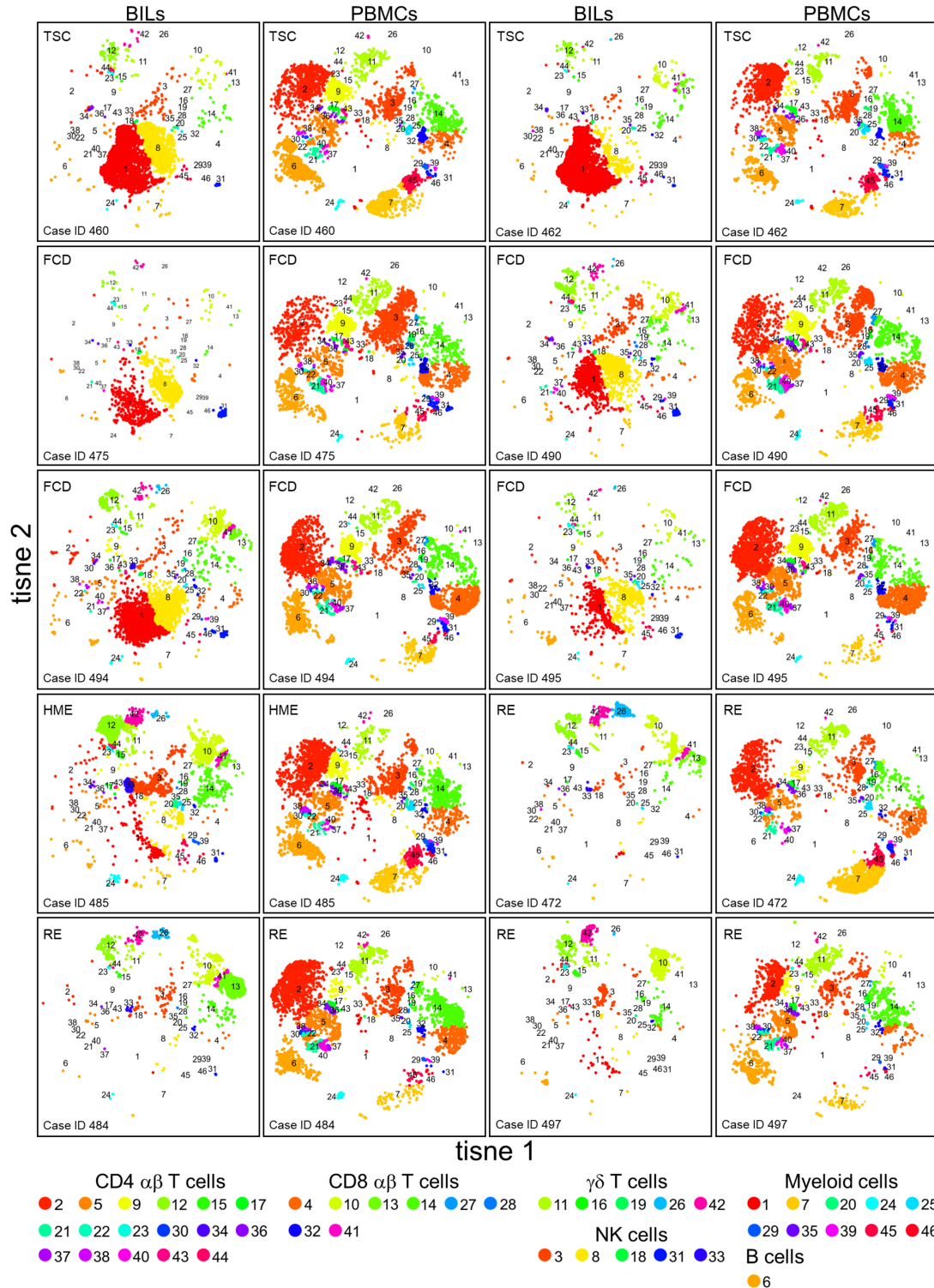
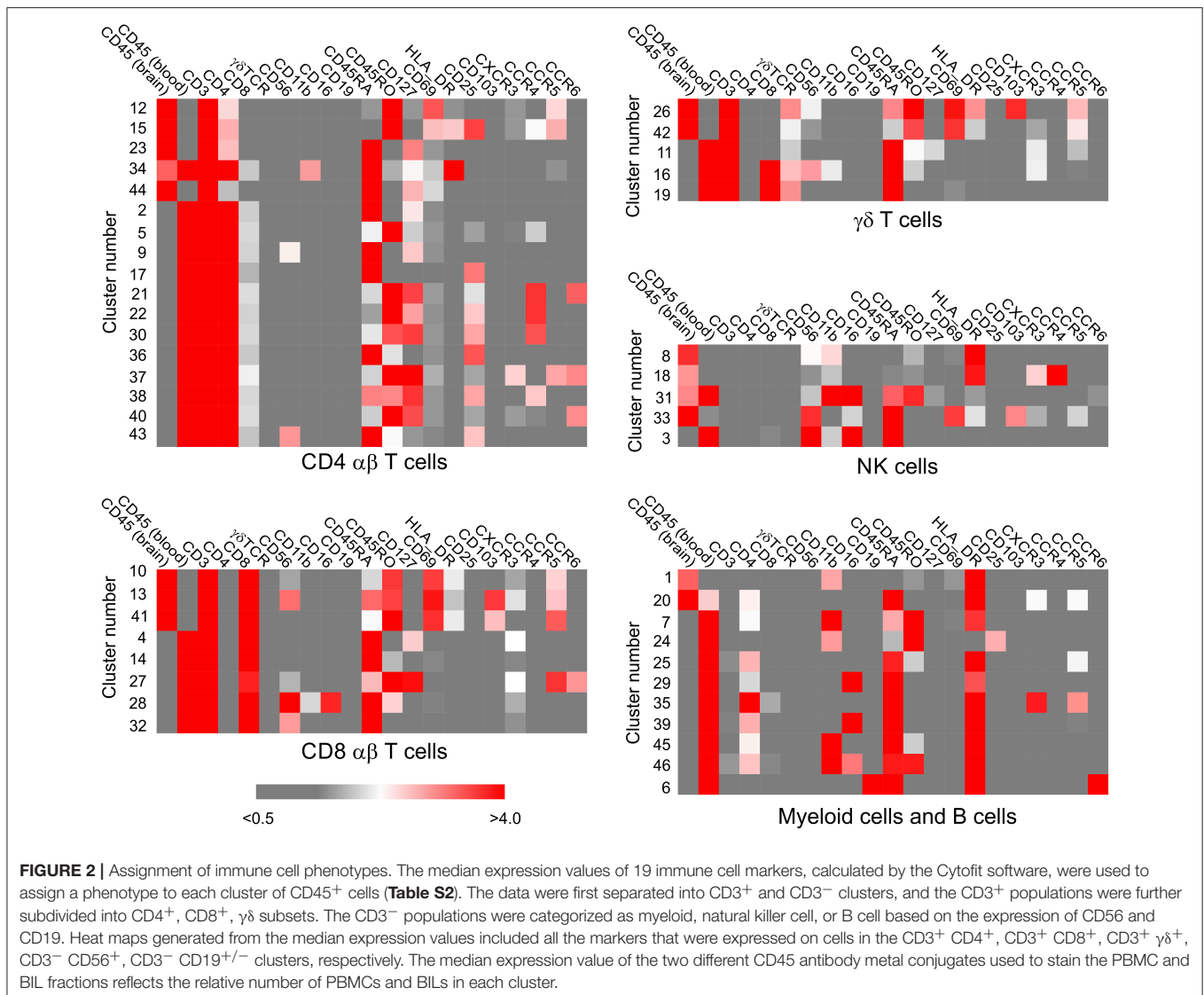


FIGURE 1 | tSNE plots showing the relative number of different immune cells in BILs and PBMCs from the pediatric epilepsy surgeries. The expression of 20 immune cell markers was analyzed by CyTOF. To define subsets of CD4⁺ cells in each BIL and PBMC population, the entire high dimensional dataset (comprising 20 FCS files) was converted into a matrix of pair-wise similarities by implementing the t-based stochastic neighbor embedding (t-SNE) algorithm, followed by a density-based clustering method (ClusterX). The clusters were assigned as either T cells, NK cells, myeloid cells, or B cells based on the median expression values of specific immune cell markers (CD3, CD4, CD8, TCR $\gamma\delta$, CD11b, CD56, and CD19).



and 8 NK cell populations by manually curating the original FCS files from FCD case 490 using the FlowJO software package (Figure S1A).

Six subpopulations of CD4⁺ $\alpha\beta$ T cells (Clusters 2, 5, 9, 12, 15, and 23), four of CD8⁺ $\alpha\beta$ T cells (Clusters 4, 10, 13, and 14), and three subsets of $\gamma\delta$ T cells (Clusters 11, 26, and 42) accounted for over 80% of the CD3⁺ T cells in all of the BIL and PBMC samples, although there were marked differences in the proportion of the different T cell subsets between the BIL and PBMC samples (Figure 5; Table S4). Clusters 2, 9 and 23 CD4⁺ T cells constitute naive T cell populations (CD45RA⁺ CD45RO⁻ CD127^{int}) (Figure 2); different median levels of expression of CD4 and CD127 appear to account for the generation of two clusters of naive conventional T cells (Clusters 2 and 23), whereas expression of CD56 by Cluster 9 CD45RA⁺ CD45RO⁻ CD4⁺ T cells indicates that they may be unconventional NKT cells.

Clusters 5 and 15 define two different subpopulations of antigen-experienced CCR4⁺ CD4⁺ T cells (Figure 2). Based on

the expression of CD25, the interleukin-2 receptor α chain (IL-2R) and lack of CD127, the interleukin-7 receptor α chain (IL-7R), Cluster 15 cells appear to be conventional regulatory T cells (Tregs) (24), and were found almost exclusively in the BIL fractions (Figure 5). Additional minor populations of CD45RO⁺ CD25⁺ CCR4⁺ CD4 T cells (Clusters 21, 22, 30, and 38) found predominantly in the blood may also be Tregs (Figure 2). Cluster 5 CD4 cells were found in both the brain and blood, and may be both IL-7 and IL-2 dependent (Figures 2, 5). Cluster 12 defined an activated effector memory population of CD4 T cells (CD45RO⁺ HLA-DR⁺ CD69⁺) (Figure 2) that was found in all of the BIL fractions (Figure 5). These cells also expressed the chemokine receptors CXCR3 and CCR5 thus may have trafficked to the epileptogenic brain area that was resected, possibly due to local inflammation (25).

Cluster 4 CD8 T cells were primarily found in the PBMC fractions and appear to correspond to an activated unprimed subtype (CD45RA⁺ CD127⁺) since they also expressed the

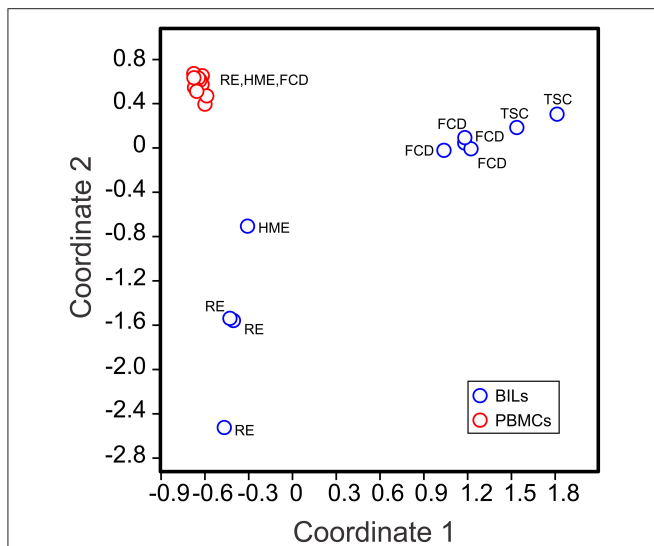


FIGURE 3 | Clustering of BILs and PBMCs from pediatric epilepsy surgeries. The relative number of cells in each cluster in each sample (as a percentage of the total number of CD45⁺ cells analyzed in each sample) was used to implement a principal component analysis (PCA). The first two components could account for 65.72% of the total variance in the data set. The 2D PCA plot shows that the BIL fractions are clearly different from the corresponding PBMCs, and that BILs from the RE and HME cases are distinct from those from the FCD and TSC cases.

chemokine receptor CXCR3 (26). A CD45RA⁺ CD45RO^{lo} subpopulation (Cluster 14) made up most of the remaining CD8 T cells in the blood (Figures 2, 5; Table S4). Cells in Clusters 10 and 13 appear to be activated (CD69⁺ HLA-DR⁺) effector memory subtypes, and were found almost exclusively in the brain (Figures 2, 5). Based on the marker panel used in this study, the only difference between these two clusters was the expression of the resident memory marker CD103. Fewer Cluster 13 CD8⁺ resident memory T cells (T_{RM}) were found in the brain compared with Cluster 10 T cells with one exception, Case ID 484, a RE patient. In agreement with previous work (27), the majority of the CD8⁺ T cells isolated from resected brain tissue from this patient were T_{RM} cells. Likewise, the majority of $\gamma\delta$ T cells isolated from a second RE case (Case ID 472) were T_{RM} cells (Cluster 26, Figure 5) (27). Cluster 26 and Cluster 42 $\gamma\delta$ T cells expressed the activation markers CD69 and HLA-DR and were almost exclusively found the brain (Figures 2, 5). These two activated subsets comprised 88–98 percent of the $\gamma\delta$ T cells in the RE BIL fractions, whereas a third subset, Cluster 11, a CCR5⁺ CXCR3⁺ effector memory population (CD45RA⁺ CD45RO^{int} CD127⁺) contributed up 70 percent of the $\gamma\delta$ T cells in the other cases (Table S4). The Cluster 11 subset also made up the vast majority of $\gamma\delta$ T cells in the blood from all of the cases (Figure 5). We verified the existence of all of the major T cell populations defined by the ClusterX clustering algorithm by manually curating several of the original FCS files (Figures S1B–D).

The donut plots in Figure 6 summarize the proportion of CD69⁺ HLA-DR⁺ T cells found in each of the BIL fractions from

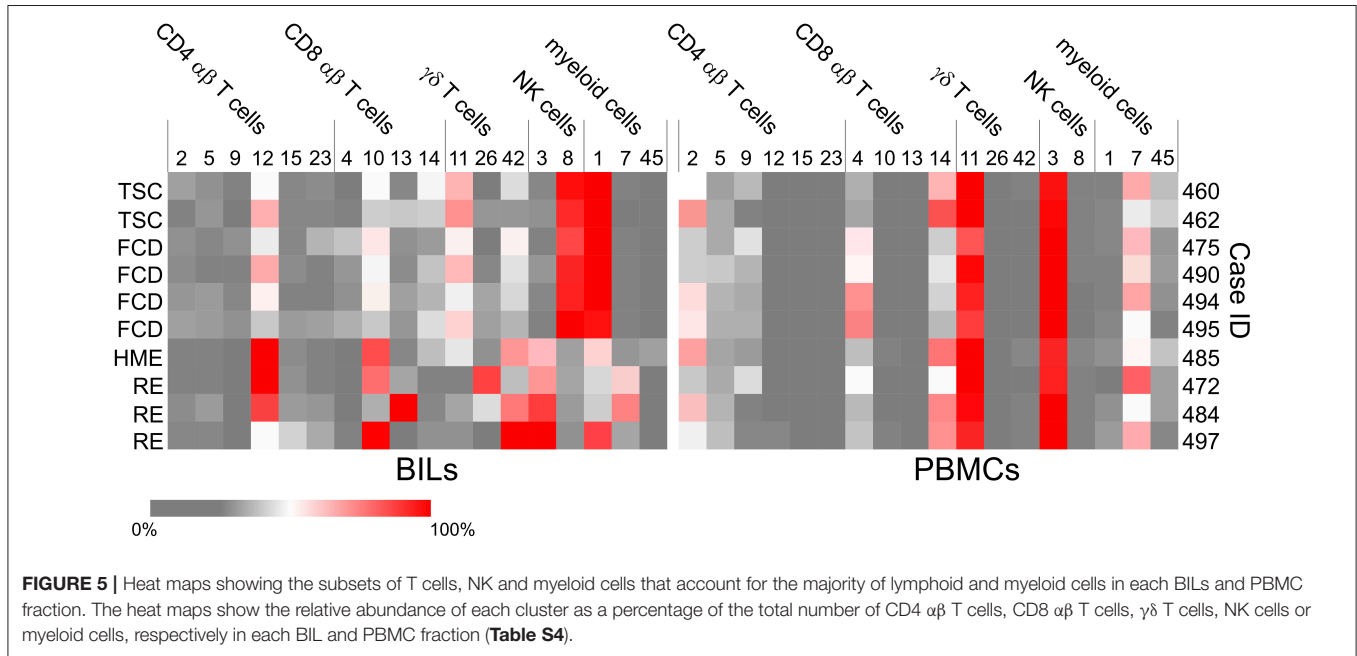
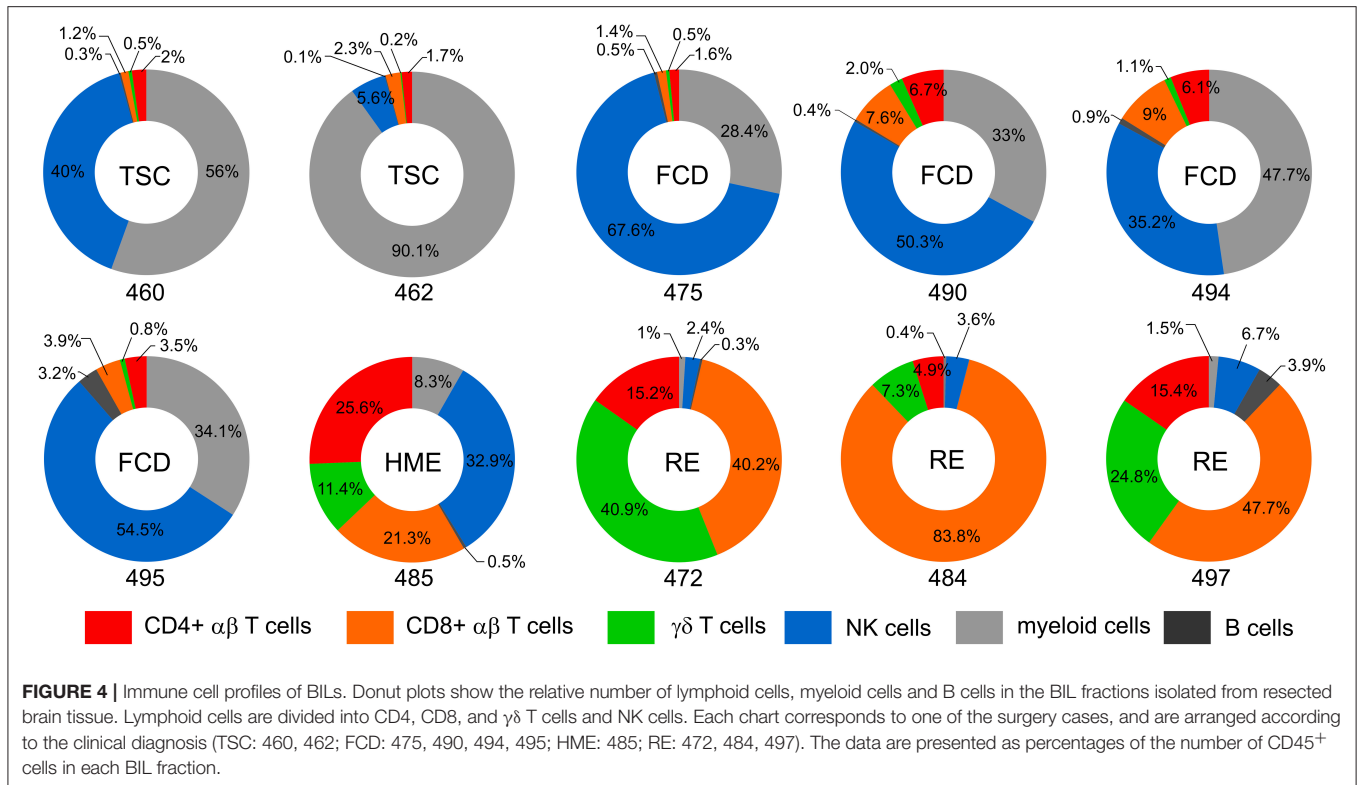
the 10 surgery cases. At least 90 percent of the T cells isolated from the RE cases and 80 percent of the T cells from the HME case were activated. Even though T cells made up only a small fraction of the CD45⁺ cells isolated from the TSC and FCD cases, 40–66 percent of the T cells were also activated at the time of surgery.

The absence of CD8⁺ T_{RM} cells in the BIL fraction from RE case ID 497 suggested that the disease may not have progressed as far in this patient compared with the other two RE cases in the study cohort (Cases IDs 472 and 484). A [¹⁸F]-deoxyglucose positron emission tomography (FDG-PET) brain scan of the patient made before the surgery showed hypometabolism extending over the entire affected hemisphere, with no definitive areas of atrophy. In the other two RE cases, areas of atrophy were clearly visible (Figure 7). Case ID 497 was the youngest of the three RE patients at the time of seizure onset and underwent surgery after the shortest time following onset of seizures (Table S1).

DISCUSSION

We have used CyTOF to gain a better understanding of the involvement of peripheral immune cells in intractable epilepsy in children. We implemented an unsupervised clustering method to resolve the resulting high dimensional data into the main subtypes of adaptive and innate lymphoid cells present in resected epileptogenic brain tissue. Our small cohort study, and other recent work (28) implicate cellular immunity not only in RE, but in intractable epilepsy in children where an infection or immune disorder is not suspected. With the caveat that we only analyzed a limited number of surgery cases, we found a clear difference in the relative number of innate vs. adaptive peripheral immune cells in fractions of CD45⁺ cells isolated from resected TSC and FCD brain tissue compared with involved RE brain tissue. The FCD and TSC BIL fractions were dominated by a single subset of NK cells (Cluster 8) and a population of myeloid cells (Cluster 1) that are likely to be macrophages, possibly classically activated pro-inflammatory M1 macrophages. Adding CD38 and CD163 antibodies to the staining panel will allow us to distinguish between M1 and M2 macrophages, respectively (29, 30). In an animal seizure model, infiltrating monocytes were shown to exacerbate neuronal damage (31), indicating that the abundant myeloid population that we found in the FCD and TSC BIL fractions may be pathologically relevant.

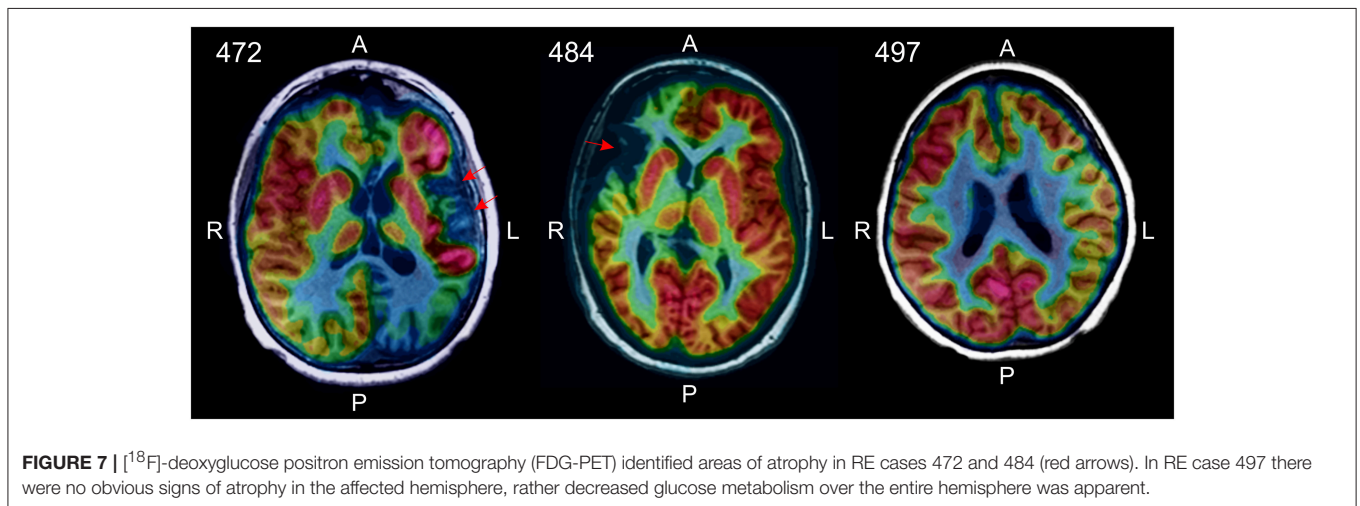
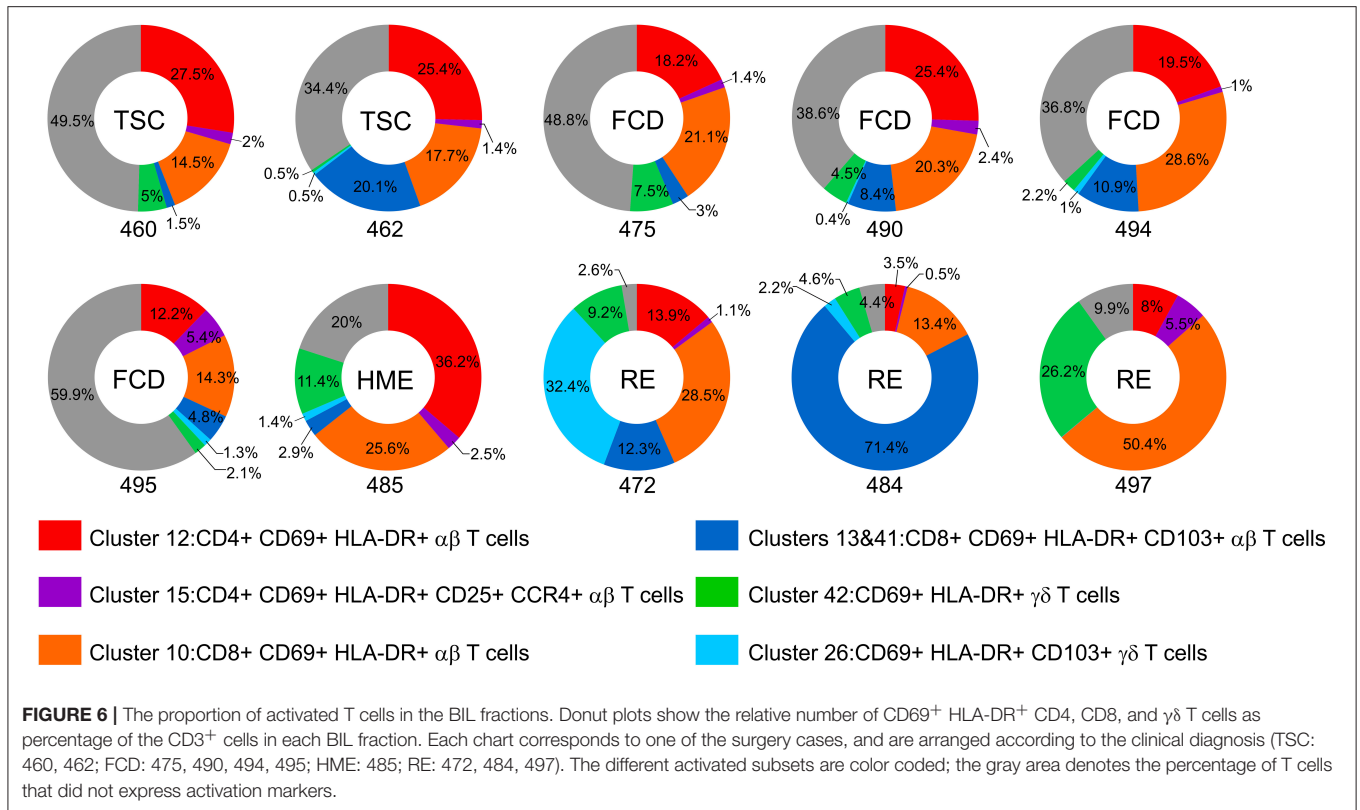
Most NK cells in the blood express a low level of CD56 (CD56^{dim}) and are CD16⁺, thus can engage in antibody-dependent cell-mediated cytotoxicity by binding antibody-coated target cells via the low affinity Fc γ receptor III (CD16) (32). Fewer circulating NK cells express a high level of CD56 (CD56^{bright}); these cells generally lack CD16, but can produce pro- or anti-inflammatory cytokines (32). CD56^{bright} NK cells are considered to be more immature than CD56^{dim} NK cells in that they mostly do not express killer cell immunoglobulin-like receptors (KIRs) (33). Unlike CD56^{dim} NK cells they express CD62L (L-selectin) and CD197 (CCR7), cell surface molecules that facilitate homing to secondary lymph nodes (32). CD56^{dim}



NK cells express KIRs and CD57 and are considered to be intrinsically more cytotoxic (32, 33). The most abundant NK cells that we found in the blood of all of the patients in our study cohort presumably correspond to CD56^{dim}CD16⁺ NK cells (Cluster 3). This subset also comprised the majority of NK cells present in the BIL fractions from the RE and HME patients (Figure 5). Adding CD62L, CD197, and CD57

to the marker panel will clarify the phenotype of Cluster 3 NK cells.

By comparison to the NK cells in the PBMC fractions, the majority of NK cells found in the FCD and TSC BIL fractions expressed a lower level of CD56 suggesting that they correspond to a CD56^{dim} subset (Cluster 8) (Figure 2, Figure S1A). Unlike canonical CD56^{dim} NK cells, Cluster 8 cells did not express



CD16, however populations of CD56^{dim} NK cells expressing little or no CD16 have been previously described (34). Lack of CD16 may be due to the fact that the Cluster 8 NK cells were highly activated; it has been reported that the Fc γ receptor III is proteolytically cleaved in degranulating CD56^{dim} NK cells (35). In contrast to Cluster 3 NK cells, Cluster 8 NK cells also expressed HLA-DR (**Figure 2, Figure S1A**), which suggests that they may be adaptive NK cells (32, 33). A third population of NK cells (Cluster 33), only found in appreciable numbers in BILs from the HME case (Case ID 485) expressed CD69 along with CCR5, CXCR3, and CD103 suggesting that

this cluster may correspond to an activated resident subset (32).

BIL fractions from the RE cases were predominantly CD8 $\alpha\beta$ and $\gamma\delta$ effector memory and resident memory T cells with fewer effector memory CD4 T cells, confirming previous work (20, 27). We and others have shown that T cells found in RE brain are clonally focused (7–10), which strongly implicates an antigen-driven adaptive immune response in the etiology of RE, and is consonant with the idea that RE is an autoimmune disease (36). Finding T_{RM} CD8 $\alpha\beta$ and $\gamma\delta$ T cells in affected RE brain tissue indicates that an earlier immune response had occurred that left

a resident memory population in place. Compared with RE cases 472 and 484 however, no T_{RM} cells were present in the BILs isolated from RE case 497, suggesting that this case may represent an early stage of the disease. In support of this idea, brain atrophy, a feature of late phases of the disease (4), was not evident in an FDG-PET brain scan of RE case 497, but was in RE cases 472 and 484 (Figure 7).

In pathological specimens from FCD and TSC surgeries scattered T cells have been previously observed (16, 17), and in our study we found activated CD4, CD8, and $\gamma\delta$ T cells in the BIL fractions from the FCD and TSC cases (Figure 6). Determining the clonal diversity of these T cells by sequencing V β chain third complementarity determining regions may indicate whether they are unspecific bystanders or presage an adaptive response against self-antigens. Binding of self-peptides would however depend on the MHC alleles carried by the individual (37–39). The proportion of activated T cells in the single HME case (Case ID 485), which exceeded the number of NK cells (Figure 4), may indicate that an autoimmune response had already occurred in this very young patient who suffered from severe seizures. Future recall assays in which T cells isolated from resected brain tissue are cocultured with autologous neurons and glia differentiated from patient-derived induced pluripotent stems cells will directly answer whether the T cells are autoreactive.

The immune cell profiles of peripheral blood from all of the cases comprised both naïve and antigen experienced T cells. $\gamma\delta$ T cells that were CD127⁺, CD45RO⁺, CXCR3⁺, and CCR5⁺ comprised the majority of $\gamma\delta$ T cells in all of the PBMC samples, as well as in the FCD and TSC BILs (Cluster 11; Figures 2, 5, Figure S1D). They likely express V δ 2/V γ 9 TCR receptors (40) since V δ 2/V γ 9 $\gamma\delta$ T cells make up a large fraction of circulating $\gamma\delta$ T cells (41). Expression of CXCR3 and CCR5 would allow these $\gamma\delta$ T cells to access sites of inflammation (26). CXCR3 expression by naïve CD45RA⁺ CD8 T cells (Cluster 4; Figure 2, Figure S1C) indicates that they are activated (42), and that development into effector T cells may be enhanced (43, 44). Whether the presence of these T cell subsets in the blood is directly related to inflammation in the brain remains to be determined. In future work we plan to compare the immune cell profiles of blood collected at the time of surgery and after recovery from surgery. Removal of epileptogenic brain tissue, the potential source of inflammation may change the relative frequency of specific circulating T cell subsets. Such subsets could potentially be used as biomarkers to assess the extent brain inflammation in children presenting with intractable epilepsy.

The distribution of the two most abundant CCR4⁺ CD4 T cell subsets (Clusters 5 and 15) differed between the blood and brain. Cluster 15 cells were almost exclusively found in BIL fractions, and appear to be activated effector memory-like Tregs (CD25⁺ CD45RO⁺CD69⁺HLA-DR⁺) (Figures 2, 5, Figure S1B). Tregs are also defined by expression of the transcription factor FOXP3 (24); adding this intracellular marker to the CyTOF panel will confirm the identity of these CD4 T cells. In a cohort of pediatric epilepsy surgery patients, a negative correlation between seizure frequency and the relative number of Tregs in resected epileptogenic brain was recently reported

(28). In our study cohort, the relative number of Cluster 15 Tregs cells ranged from 2.61 to 31.53 percent of CD4 T cells in the BIL fractions (Table S4). However, the limited number of self-reports of seizure activity available do not allow us to draw any conclusions about the number of seizures and the percent Tregs in our patient cohort. Cluster 5 CD45RO⁺CCR4⁺ CD4 T cells (Figure 2, Figure S1B), which express both IL-2Rs and IL-7Rs, were found in both BIL and PBMC fractions, and may correspond to a subset of CD4 T cells that express CD25 and CD127 and low levels of FOXP3, and are not suppressive *in vitro* (24). Adding the FOXP3 Ab to the marker panel may help clarify the identity of this subset of CD4 T cells.

Extensive animal studies have shown that inflammation in the brain is both a cause and a consequence of seizure activity (45). Attention has focused on the innate response of brain resident microglia and astrocytes to seizures and on the pro-inflammatory molecules produced by these cells as drivers of epileptogenesis (46–48). In seizure models, chemokines and cytokines produced by activated microglia and astrocytes can cause blood brain barrier leakage, and can attract peripheral lymphoid and myeloid cells to the brain (31, 49–51). Our data suggest that this could be happening in children with chronic pharmacoresistant seizures. Intractable epilepsy might be viewed as a “sterile” infection in which T cells and other immune cells traffic to epileptogenic areas of the cerebral cortex in response to local seizure-driven inflammation. Activated T cells and NK cells for example could permanently alter brain circuitry by directly or indirectly damaging neurons (52–55). Adjunctive treatments that block the recruitment of pro-inflammatory peripheral lymphoid and myeloid cells to the brain (56–61) may therefore be therapeutically beneficial.

AUTHOR CONTRIBUTIONS

GO designed the study, analyzed the data, and wrote the paper. AG assisted with study design and performed the CyTOF. AM assisted with analysis of the data. JC and SR coordinated collection of surgical specimens and prepared BILs and PBMCs. RP assisted with study design and helped draft the paper. NS provided FDG-PET results. GM supported the project. AF provided support for the work, and provided surgical specimens and patient information.

ACKNOWLEDGMENTS

This work was supported by The RE Children’s Project and NIH/NCATS/UCLA CTSI UL1TR001881, and in part by NIH R01 NS083823 and U01 MH108898. GM was partly supported by the Davies/Crandall Endowed Chair for Epilepsy Research at UCLA.

SUPPLEMENTARY MATERIAL

The Supplementary Material for this article can be found online at: <https://www.frontiersin.org/articles/10.3389/fimmu.2019.00121/full#supplementary-material>

REFERENCES

- Guerrini R. Epilepsy in children. *Lancet* (2006) 367:499–524. doi: 10.1016/S0140-6736(06)68182-8
- Berg AT, Kelly MM. Defining intractability: comparisons among published definitions. *Epilepsia* (2006) 47:431–6. doi: 10.1111/j.1528-1167.2006.00440.x
- Varadkar S, Bien CG, Kruse CA, Jensen FE, Bauer J, Pardo CA, et al. Rasmussen's encephalitis: clinical features, pathobiology, and treatment advances. *Lancet Neurol.* (2014) 13:195–205. doi: 10.1016/S1474-4422(13)70260-6
- Bien CG, Urbach H, Deckert M, Schramm J, Wiestler OD, Lassmann H, et al. Diagnosis and staging of Rasmussen's encephalitis by serial MRI and histopathology. *Neurology* (2002) 58:250–7. doi: 10.1212/WNL.58.2.250
- Prayson RA, Frater JL. Rasmussen encephalitis: a clinicopathologic and immunohistochemical study of seven patients. *Am J Clin Pathol.* (2002) 117:776–82. doi: 10.1309/AD8R-560C-4V11-C5E2
- Pardo CA, Vining EP, Guo L, Skolasky RL, Carson BS, Freeman JM. The pathology of Rasmussen syndrome: stages of cortical involvement and neuropathological studies in 45 hemispherectomies. *Epilepsia* (2004) 45:516–26. doi: 10.1111/j.0013-9580.2004.33103.x
- Schwab N, Bien CG, Waschbisch A, Becker A, Vince GH, Dornmair K, et al. CD8+ T-cell clones dominate brain infiltrates in Rasmussen encephalitis and persist in the periphery. *Brain* (2009) 132:1236–46. doi: 10.1093/brain/awp003
- Schneider-Hohendorf T, Mohan H, Bien CG, Breuer J, Becker A, Gorlich D, et al. CD8(+) T-cell pathogenicity in Rasmussen encephalitis elucidated by large-scale T-cell receptor sequencing. *Nat Commun.* (2016) 7:11153. doi: 10.1038/ncomms11153
- Dandekar S, Wijesuriya H, Geiger T, Hamm D, Mathern GW, Owens GC. Shared HLA CLASS I and II alleles and clonally restricted public and private brain-infiltrating alpha beta T cells in a cohort of Rasmussen encephalitis surgery patients. *Front Immunol.* (2016) 7:608. doi: 10.3389/fimmu.2016.00608
- Al Nimer F, Jelcic I, Kempf C, Pieper T, Budka H, Sospedra M, et al. Phenotypic and functional complexity of brain-infiltrating T cells in Rasmussen encephalitis. *Neurol Neuroimmunol Neuroinflamm.* (2018) 5:e419. doi: 10.1212/NXI.0000000000000419
- Martin KR, Zhou W, Bowman MJ, Shih J, Au KS, Dittenhafer-Reed KE, et al. The genomic landscape of tuberous sclerosis complex. *Nat Commun.* (2017) 8:15816. doi: 10.1038/ncomms15816
- Polchi A, Magini A, Meo DD, Tancini B, Emiliani C. mTOR signaling and neural stem cells: the tuberous sclerosis complex model. *Int J Mol Sci.* (2017) 19:E1474. doi: 10.3390/ijms19051474
- Mirzaa GM, Campbell CD, Solovieff N, Goold C, Jansen LA, Menon S, et al. Association of MTOR mutations with developmental brain disorders, including megalencephaly, focal cortical dysplasia, and pigmentary mosaicism. *JAMA Neurol.* (2016) 73:836–45. doi: 10.1001/jamaneurol.2016.0363
- D'Gama AM, Woodworth MB, Hossain AA, Bizzotto S, Hatem NE, LaCoursiere CM, et al. Somatic mutations activating the mTOR pathway in dorsal telencephalic progenitors cause a continuum of cortical dysplasias. *Cell Rep.* (2017) 21:3754–766. doi: 10.1016/j.celrep.2017.11.106
- Alcantara D, Timms AE, Gripp K, Baker L, Park K, Collins S, et al. Mutations of AKT3 are associated with a wide spectrum of developmental disorders including extreme megalencephaly. *Brain* (2017) 140:2610–22. doi: 10.1093/brain/awx203
- Boer K, Jansen F, Nellist M, Redeker S, van den Ouweland AM, Spliet WG, et al. Inflammatory processes in cortical tubers and subependymal giant cell tumors of tuberous sclerosis complex. *Epilepsy Res.* (2008) 78:7–21. doi: 10.1016/j.eplepsyres.2007.10.002
- Iyer A, Zurolo E, Spliet WG, van Rijen PC, Baayen JC, Gorter JA, et al. Evaluation of the innate and adaptive immunity in type I and type II focal cortical dysplasias. *Epilepsia* (2010) 51:1763–73. doi: 10.1111/j.1528-1167.2010.02547.x
- Boer K, Crino PB, Gorter JA, Nellist M, Jansen FE, Spliet WG, et al. Gene expression analysis of tuberous sclerosis complex cortical tubers reveals increased expression of adhesion and inflammatory factors. *Brain Pathol.* (2010) 20:704–19. doi: 10.1111/j.1750-3639.2009.00341.x
- Prabowo AS, Anink JJ, Lammens M, Nellist M, van den Ouweland AM, Adle-Biasette H, et al. Fetal brain lesions in tuberous sclerosis complex: TORC1 activation and inflammation. *Brain Pathol.* (2013) 23:45–59. doi: 10.1111/j.1750-3639.2012.00616.x
- Owens GC, Erickson KL, Malone CC, Pan C, Huynh MN, Chang JW, et al. Evidence for the involvement of gamma delta T cells in the immune response in Rasmussen encephalitis. *J Neuroinflammation* (2015) 12:134. doi: 10.1186/s12974-015-0352-2
- Chen TJ, Kotecha N. Cytobank: providing an analytics platform for community cytometry data analysis and collaboration. *Curr Top Microbiol Immunol.* (2014) 377:127–57. doi: 10.1007/82_2014_364
- Chen H, Lau MC, Wong MT, Newell EW, Poidinger M, Chen, J. Cytokit: a bioconductor package for an integrated mass cytometry data analysis pipeline. *PLoS Comput Biol.* (2016) 12:e1005112. doi: 10.1371/journal.pcbi.1005112
- Bien CG, Bauer J, Deckwerth TL, Wiendl H, Deckert M, Wiestler OD, et al. Destruction of neurons by cytotoxic T cells: a new pathogenic mechanism in Rasmussen's encephalitis. *Ann Neurol.* (2002) 51:311–8. doi: 10.1002/ana.10100
- Sakaguchi S, Miyara M, Costantino CM, Hafler DA. FOXP3+ regulatory T cells in the human immune system. *Nat Rev Immunol.* (2010) 10:490–500. doi: 10.1038/nri2785
- Trebst C, Staugaitis SM, Tucky B, Wei T, Suzuki K, Aldape KD, et al. Chemokine receptors on infiltrating leucocytes in inflammatory pathologies of the central nervous system (CNS). *Neuropathol Appl Neurobiol.* (2003) 29:584–95. doi: 10.1046/j.0305-1846.2003.00507.x
- Groom JR, Luster AD. CXCR3 in T cell function. *Exp Cell Res.* (2011) 317:620–31. doi: 10.1016/j.yexcr.2010.12.017
- Owens GC, Chang JW, Huynh MN, Chirwa T, Vinters HV, Mathern GW. Evidence for resident memory T cells in Rasmussen encephalitis. *Front Immunol.* (2016) 7:64. doi: 10.3389/fimmu.2016.00064
- Xu D, Robinson AP, Ishii T, Duncan DS, Alden TD, Goings GE, et al. Peripherally derived T regulatory and gammadelta T cells have opposing roles in the pathogenesis of intractable pediatric epilepsy. *J Exp Med.* (2018) 215:1169–86. doi: 10.1084/jem.20171285
- Zwadlo G, Voegeli R, Schulze Osthoff K, Sorg C, A monoclonal antibody to a novel differentiation antigen on human macrophages associated with the down-regulatory phase of the inflammatory process. *Exp Cell Biol.* (1987) 55:295–304.
- Amici SA, Young NA, Narvaez-Miranda J, Jablonski KA, Arcos J, Rosas, L, et al. CD38 is robustly induced in human macrophages and monocytes in inflammatory conditions. *Front Immunol.* (2018) 9:1593. doi: 10.3389/fimmu.2018.01593
- Varvel NH, Neher JJ, Bosch A, Wang W, Ransohoff RM, Miller RJ, et al. Infiltrating monocytes promote brain inflammation and exacerbate neuronal damage after status epilepticus. *Proc Natl Acad Sci USA.* (2016) 113:E5665–74. doi: 10.1073/pnas.1604263113
- Cichicki F, Schlums H, Theorell J, Tesi B, Miller JS, Ljunggren HG, et al. Diversification and functional specialization of human NK cell subsets. *Curr Top Microbiol Immunol.* (2016) 395:63–94. doi: 10.1007/82_2015_487
- Freud AG, Mundy-Bosse BL, Yu J, Caligiuri MA. The broad spectrum of human natural killer cell diversity. *Immunity* (2017) 47:820–33. doi: 10.1016/j.immuni.2017.10.008
- Amand M, Iserentant G, Poli A, Sleiman M, Fievez V, Sanchez IP, et al. Human CD56(dim)CD16(dim) cells as an individualized natural killer cell subset. *Front Immunol.* (2017) 8:699. doi: 10.3389/fimmu.2017.00699
- Lajoie L, Congy-Jolivet N, Bolzec A, Gouilleux-Gruart V, Sicard, E, Sung HC, et al. ADAM17-mediated shedding of Fc gammaRIIIA on human NK cells: identification of the cleavage site and relationship with activation. *J Immunol.* (2014) 192:741–51. doi: 10.4049/jimmunol.1301024
- Amrom D, Kinay D, Hart Y, Berkovic SF, Laxer K, Andermann F, et al. Rasmussen encephalitis and comorbid autoimmune diseases: a window into disease mechanism? *Neurology* (2014) 83:1049–55. doi: 10.1212/WNL.0000000000000791
- Gough SC, Simmonds MJ. The HLA region and autoimmune disease: associations and mechanisms of action. *Curr Genomics* (2007) 8:453–65.
- Miyadera H, Tokunaga K. Associations of human leukocyte antigens with autoimmune diseases: challenges in identifying the mechanism. *J Hum Genet.* (2015) 60:697–702. doi: 10.1038/jhg.2015.100

39. Gutierrez-Arcelus M, Rich SS, Raychaudhuri S. Autoimmune diseases - connecting risk alleles with molecular traits of the immune system. *Nat Rev Genet.* (2016) 17:160–74. doi: 10.1038/nrg.2015.33
40. Glatzel A, Wesch D, Schiemann F, Brandt E, Janssen O, Kabelitz D. Patterns of chemokine receptor expression on peripheral blood gamma delta T lymphocytes: strong expression of CCR5 is a selective feature of V delta 2/V gamma 9 gamma delta T cells. *J Immunol.* (2002) 168:4920–9. doi: 10.4049/jimmunol.168.10.4920
41. Pang DJ, Neves JF, Sumaria N, Pennington DJ. Understanding the complexity of gammadelta T-cell subsets in mouse and human. *Immunology* (2012) 136:283–90. doi: 10.1111/j.1365-2567.2012.03582.x
42. Groom JR, Luster AD. CXCR3 ligands: redundant, collaborative and antagonistic functions. *Immunol Cell Biol.* (2011) 89:207–15. doi: 10.1038/icb.2010.158
43. Kurachi M, Kurachi J, Suenaga F, Tsukui T, Abe J, Ueha S, et al. Chemokine receptor CXCR3 facilitates CD8(+) T cell differentiation into short-lived effector cells leading to memory degeneration. *J Exp Med.* (2011) 208:1605–20. doi: 10.1084/jem.20102101
44. Groom JR, Richmond J, Murooka TT, Sorensen EW, Sung JH, Bankert K, et al. CXCR3 chemokine receptor-ligand interactions in the lymph node optimize CD4+ T helper 1 cell differentiation. *Immunity* (2012) 37:1091–103. doi: 10.1016/j.immuni.2012.08.016
45. Vezzani A, French J, Bartfai T, Baram TZ. The role of inflammation in epilepsy. *Nat Rev Neurol.* (2011) 7:31–40. doi: 10.1038/nrneurol.2010.178
46. Vezzani A, Auvin S, Ravizza T, Aronica E. Glia-neuronal interactions in ictogenesis and epileptogenesis: role of inflammatory mediators. In: Noebels JL, Avoli M, Rogawski MA, Olsen RW, Delgado-Escueta AV, editors. *Jasper's Basic Mechanisms of the Epilepsies*. Bethesda, MD: Oxford University Press (2012).
47. Devinsky O, Vezzani A, Najjar S, De Lanerolle NC, Rogawski MA. Glia and epilepsy: excitability and inflammation. *Trends Neurosci.* (2013) 36:174–84. doi: 10.1016/j.tins.2012.11.008
48. Eyo UB, Murugan M, Wu LJ. Microglia-neuron communication in epilepsy. *Glia* (2017) 65:5–18. doi: 10.1002/glia.23006
49. Vezzani A, Ravizza T, Balosso S, Aronica E. Glia as a source of cytokines: implications for neuronal excitability and survival. *Epilepsia* (2008) 49 (Suppl. 2):24–32. doi: 10.1111/j.1528-1167.2008.01490.x
50. Fabene PF, Bramanti P, Constantin G. The emerging role for chemokines in epilepsy. *J Neuroimmunol.* (2010) 224:22–7. doi: 10.1016/j.jneuroim.2010.05.016
51. Fabene PF, Laudanna C, Constantin G. Leukocyte trafficking mechanisms in epilepsy. *Mol Immunol.* (2013) 55:100–4. doi: 10.1016/j.molimm.2012.12.009
52. Melzer N, Meuth SG, Wiendl H. CD8+ T cells and neuronal damage: direct and collateral mechanisms of cytotoxicity and impaired electrical excitability. *Faseb J.* (2009) 23:3659–73. doi: 10.1096/fj.09-136200
53. Kreutzfeldt M, Bergthaler A, Fernandez M, Bruck W, Steinbach K, Vorm M, et al. Neuroprotective intervention by interferon-gamma blockade prevents CD8+ T cell-mediated dendrite and synapse loss. *J Exp Med.* (2013) 210:2087–103. doi: 10.1084/jem.20122143
54. Ehling P, Melzer N, Budde T, Meuth SG. CD8(+) T cell-mediated neuronal dysfunction and degeneration in limbic encephalitis. *Front Neurol.* (2015) 6:163. doi: 10.3389/fneur.2015.00163
55. Di Liberto G, Pantelyushin S, Kreutzfeldt M, Page N, Musardo S, Coras R, et al. Neurons under T cell attack coordinate phagocyte-mediated synaptic stripping. *Cell* (2018) 175:458–471 e19. doi: 10.1016/j.cell.2018.07.049
56. Sotgiu S, Murrighile MR, Constantin G. Treatment of refractory epilepsy with natalizumab in a patient with multiple sclerosis. Case report. *BMC Neurol.* (2010) 10:84. doi: 10.1186/1471-2377-10-84
57. Bittner S, Simon OJ, Gobel K, Bien CG, Meuth SG, Wiendl H. Rasmussen encephalitis treated with natalizumab. *Neurology* (2013) 81:395–7. doi: 10.1212/WNL.0b013e31829c5ceb
58. Martin-Blondel G, Brassat D, Bauer J, Lassmann H, Liblau RS. CCR5 blockade for neuroinflammatory diseases—beyond control of HIV. *Nat Rev Neurol.* (2016) 12:95–105. doi: 10.1038/nrneurol.2015.248
59. Ayzenberg I, Hoepner R, Kleiter I. Fingolimod for multiple sclerosis and emerging indications: appropriate patient selection, safety precautions, and special considerations. *Ther Clin Risk Manag.* (2016) 12:261–72. doi: 10.2147/TCRM.S65558
60. Robert R, Juglair L, Lim EX, Ang C, Wang JH, Ebert G, et al. A fully humanized IgG-like bispecific antibody for effective dual targeting of CXCR3 and CCR6. *PLoS ONE* (2017) 12:e0184278. doi: 10.1371/journal.pone.0184278
61. Liang F, Giordano C, Shang D, Li Q, Petrof BJ. The dual CCR2/CCR5 chemokine receptor antagonist Cenicriviroc reduces macrophage infiltration and disease severity in Duchenne muscular dystrophy (Dmdmdx-4Cv) mice. *PLoS ONE* (2018) 13:e0194421. doi: 10.1371/journal.pone.0194421

Conflict of Interest Statement: The authors declare that the research was conducted in the absence of any commercial or financial relationships that could be construed as a potential conflict of interest.

Copyright © 2019 Owens, Garcia, Mochizuki, Chang, Reyes, Salamon, Prins, Mathern and Fallah. This is an open-access article distributed under the terms of the Creative Commons Attribution License (CC BY). The use, distribution or reproduction in other forums is permitted, provided the original author(s) and the copyright owner(s) are credited and that the original publication in this journal is cited, in accordance with accepted academic practice. No use, distribution or reproduction is permitted which does not comply with these terms.